Cleavage faces of wurtzite CdS and CdSe: Surface relaxation and electronic structure

Y. R. Wang and C. B. Duke
Xerox Webster Research Center, 0114-38D, 800 Phillips Road, Webster, New York 14580
(Received 14 August 1987)

The atomic geometries and electronic structures of the cleavage faces, $(10\bar{1}0)$ and $(11\bar{2}0)$, of wurtzite-structure CdS and CdSe are calculated using an sp^3 tight-binding model. The model is validated by comparison with bulk optical and x-ray photoemission data. The perpendicular displacement of the top-layer anion relative to the corresponding cation, $\Delta_{1,\perp}$, is predicted to be 0.72 Å (CdS) and 0.77 Å (CdSe) for the $(10\bar{1}0)$ surfaces, and 0.68 Å (CdS) and 0.71 Å (CdSe) for the $(11\bar{2}0)$ surfaces. The model also predicts a surface state near the top of the valence band, as well as at least four additional surface states and resonances lying within the valence band for both surfaces. Both the surface reconstructions and surface states are analogous to those predicted for other wurtzite-structure compound semiconductors. The values of $\Delta_{1,\perp}$ are shown to scale linearly with the bulk lattice constant just as for the (110) surfaces of zinc-blende-structure materials.

I. INTRODUCTION

In spite of an extensive literature on the atomic geometry[1,2] and electronic structure[2] of the (110) cleavage faces of zinc-blende-structure compound semiconductors, the $(10\bar{1}0)$ and $(11\bar{2}0)$ cleavage faces of wurtzite-structure materials have remained relatively unexplored.[2,3] In response to this situation, a series of studies of the $(10\bar{1}0)$ and $(11\bar{2}0)$ surfaces of zinc-based wurtzite-structure materials have been reported for ZnSe (Ref. 4) [for which adequate models of the electronic structure already exist[5-8] and the structure of the (110) surface of its zinc-blende allotrope is known[7,9]], ZnS (Ref. 10) [for which the atomic geometry[11] and photoemission spectra[12] of the (110) surface of its zinc-blende allotrope are given in the literature], and ZnO (Ref. 13) [for which the atomic geometry[14] and valence-electron photoemission spectra[15] characteristic of the $(10\bar{1}0)$ cleavage surface are known]. The Cd-based wurtzite-structure II-VI compounds, CdS and CdSe, are far less extensively studied. Some fragmentary low-energy electron diffraction (LEED) intensity data[3] and valence-electron photoemission spectra[16-21] have been reported in the literature. No surface-structure analysis for either the $(10\bar{1}0)$ or the $(11\bar{2}0)$ surfaces of CdS or CdSe exists, however, and the prevailing view of the photoemission spectra is that they reflect only the effects of the bulk energy-band structure,[19-21] just like the optical spectra.[22-24] Similarly, a number of calculations of the bulk energy bands of these materials have been given,[25-28] but the surface-state and surface resonance spectra remain unexamined.

Our purpose in this paper is to report the extension of the sp^3 tight-binding model[4-7,10] to CdS and CdSe, its further extension to total-surface-energy calculations,[4,5,10] and its application to calculate the surface atomic geometries and surface-state (and resonance) eigenvalue spectra of the $(10\bar{1}0)$ and $(11\bar{2}0)$ cleavage surfaces of these materials. While not as sophisticated a model as the fully self-consistent methods which have been utilized in some of the bulk-band-structure calculations,[27,28] this scheme has been applied to many comparable semiconducting materials,[4-7,10,13,29,30] and has yielded entirely satisfactory results for surface structures and surface-state energies including those of the (110) surfaces on InP and InAs which are isoelectronic with CdS and CdSe, respectively. The sp^3 tight-binding model will be validated in Sec. II by comparison with experimental optical data and x-ray photoemission. The calculations of the atomic geometry of $(10\bar{1}0)$ and $(11\bar{2}0)$ surfaces are presented in Sec. III. Using the calculated surface geometries, we then evaluate the surface electronic band structure in Sec. IV. A brief discussion is given in Sec. V.

II. THE sp^3 EMPIRICAL TIGHT-BINDING MODEL

Our sp^3 empirical tight-binding model encompasses only nearest-neighbor interactions and takes the Cd 5*s*, Cd 5*p*, S 3*s* (or Se 4*s*), and S 3*p*, (or Se 4*p*) orbitals as a basis set. The Cd 4*d* level is not included because it has a narrow bandwidth with energies about 9–10 eV below the valence-band maximum,[16-18] and hence exerts little effect either on the electronic structure near the top of the valence band or on the energetics of surface relaxation. The inclusion of the Cd 5*p* orbital is necessary for a quantitative description of surface reconstruction, as indicated from our analyses of the zinc-based compound semiconductors.[4,5,10,13]

The model has nine empirical parameters: four on-site energies and five orbital interactions. To evaluate these parameters, we compare our calculated bulk band structure with the valence-electron x-ray photoemission spectrum (XPS) (Ref. 17) and optical-transition data.[22-24] Since CdS and CdSe under normal conditions crystallize the wurtzite structure, most experiments have been done with that structure. Although it is possible to determine the parameters directly from experimental data for this structure,[13] the procedure can be simplified considerably by use of the fact that the c/a ratios of CdS (1.632) and CdSe (1.633) are almost ideal (1.633). Therefore the bonding in the wurtzite structure is essentially identical

 ©1988 The American Physical Society

TABLE I. Empirical sp^3 tight-binding interactions (in units of eV) of CdS and CdSe. The index 1 (2) refers to anion (cation); the notation is that of Slater and Koster (Ref. 33). Also given are the elastic energy parameters, U_1 and U_2, in units of eV/atom; the bulk modulus used to derive U_2 is 6.15×10^{11} dyn/cm^2 for CdS, and 5.50×10^{11} dyn/cm^2 for CdSe.

	$E_s(1)$	$E_s(2)$	$E_p(1)$	$E_p(2)$	$V_{ss\sigma}(1,2)$	$V_{sp\sigma}(1,2)$
CdS	−11.937	2.217	1.763	4.637	−0.549	0.443
CdSe	−10.960	1.360	1.640	4.560	−0.659	0.342

	$V_{sp\sigma}(2,1)$	$V_{pp\sigma}(1,2)$	$V_{pp\pi}(1,2)$	U_1	U_2
CdS	2.809	3.338	−0.597	−14.855	66.272
CdSe	2.814	3.361	−0.655	−14.953	66.872

with that in the zinc-blende allotrope. Indeed, investigations of the electronic structure properties of CdS, and the ultraviolet-reflective spectra observed in bulk wurtzite[23] and in epitaxially grown zinc-blende[22] CdS, have shown that the fundamental band gaps in both structures differ only by less than 0.1 eV. Therefore we can transform symmetry-point energies in wurtzite structure to their corresponding values in zinc-blende structure using standard assignments.[31] The tight-binding parameters can then be determined using the values of these energies for the zinc-blende structure.

The Hamiltonian matrix in the zinc-blende structure[32] is 8×8. It can be decoupled into smaller matrices at symmetry points, e.g., Γ, X, and L of the Brillioun zone. At the Γ point, we obtain the following equations:

$$64V_{ss\sigma}^2(1,2)+[E_s(2)-E_s(1)]^2=[E(\Gamma_1^c)-E(\Gamma_1^v)]^2 , \quad (1)$$

$$E_s(1)-E_s(2)=E(\Gamma_1^c)+E(\Gamma_1^v) , \quad (2)$$

$$\tfrac{64}{9}[V_{pp\sigma}(1,2)+2V_{pp\pi}(1,2)]^2 +[E_p(2)-E_p(1)]^2=E^2(\Gamma_{15}^c) , \quad (3)$$

and

$$E_p(1)+E_p(2)=E(\Gamma_{15}^c) . \quad (4)$$

Here 1 (2) stands for the anion (cation); c (v) stands for the conduction (valence) band; and other notations are those of Slater and Koster.[33] In Eqs. (3) and (4), we have set the energy of the top of the valence band, $E(\Gamma_{15}^v)$, to be zero. At the X point, the Hamiltonian matrix can be decoupled into four 2×2 matrices,

$$[E_s(1)-E(X_1^v)][E_p(2)-E(X_1^v)]=\tfrac{16}{3}V_{sp\sigma}^2(1,2) , \quad (5)$$

$$E_s(1)+E_p(2)=E(X_1^c)+E(X_1^v) , \quad (6)$$

$$[E_s(2)-E(X_3^v)][E_p(1)-E(X_3^v)]=\tfrac{16}{3}V_{sp\sigma}^2(2,1) , \quad (7)$$

and

$$[E_p(1)-E(X_5^v)][E_p(2)-E(X_5^v)] =\tfrac{16}{9}[V_{pp\sigma}(1,2)-V_{pp\pi}(1,2)]^2 . \quad (8)$$

Finally, at the L point, the matrix can be decoupled into two 4×4 matrices. One of the 4×4 matrices has a simple solution,

$$[E_p(1)-E(L_3^v)][E_p(2)-E(L_3^v)] =\tfrac{4}{9}[2V_{pp\sigma}(1,2)+V_{pp\pi}(1,2)]^2 . \quad (9)$$

These equations connect our model parameters with bulk-band energies at symmetry points for the zinc-blende structure. For CdS, $E(\Gamma_1^c)$ and $E(\Gamma_{15}^c)$ are obtained from ultraviolet-reflectivity peaks,[22] $E(\Gamma_1^c)=2.55$ eV and $E(\Gamma_{15}^c)=6.40$ eV. $E(L_3^v)=-1.10$ eV, $E(X_5^v)=2.24$ eV, and $E(X_3^v)=-4.5$ eV can be obtained from XPS measurements.[17] $E(X_1^c)=4.65$ eV is estimated from $L_{\rm II,III}$ absorption spectra.[34] This value also agrees notably well with that obtained from ultraviolet-reflectivity measurements.[35] There are no experimental data for the bottom of the valence band, $E(\Gamma_1^v)$. Calculations[27,28] indicate, however, that $E(\Gamma_1^v)\simeq-12.27$ eV. The parameters for CdS determined from Eqs. (1)–(9) are listed in Table I.

The parameters for CdSe are determined similarly. The experimental bulk band structure is specified in Table II, where $E(L_3^v)$, $E(X_5^v)$, and $E(X_3^v)$ are taken from Ref. 17, and $E(\Gamma_1^c)$ is from Ref. 23. Ultraviolet-

TABLE II. Bulk-band structure of zinc-blende CdS and CdSe from optical measurements (in eV).

CdS				CdSe			
L_3^v	−1.10	Γ_1^c	2.55	L_3^v	−1.20	Γ_1^c	1.90
X_5^v	−2.24	Γ_{15}^c	6.40	X_5^v	−2.45	Γ_{15}^c	6.25
X_3^v	−4.50	X_1^c	4.65	X_3^v	−5.1	$X_5^v\rightarrow X_1^c$	6.26
Γ_1^v	−12.27[a]	$L_3^v\rightarrow L_1^c$	5.30	Γ_1^v	−11.5[a]	$L_3^v\rightarrow L_1^c$	4.56

[a]Value from calculation or estimate.

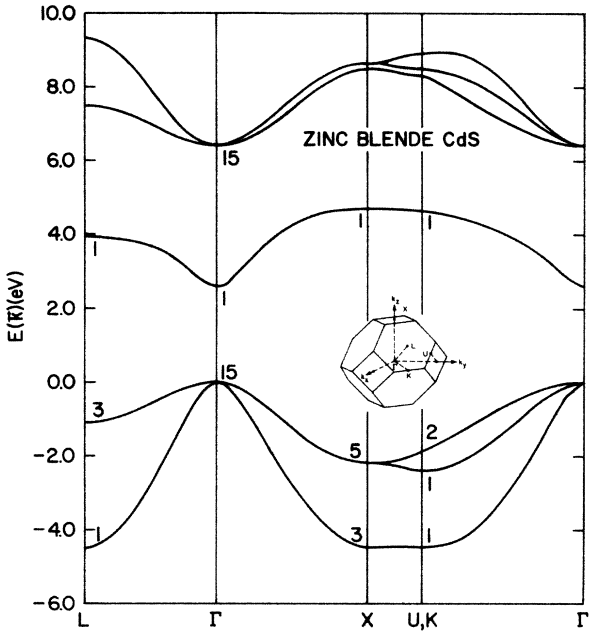

FIG. 1. Bulk-band structure of zinc-blende CdS calculated from the sp^3 model. The inset shows the Brillouin zone.

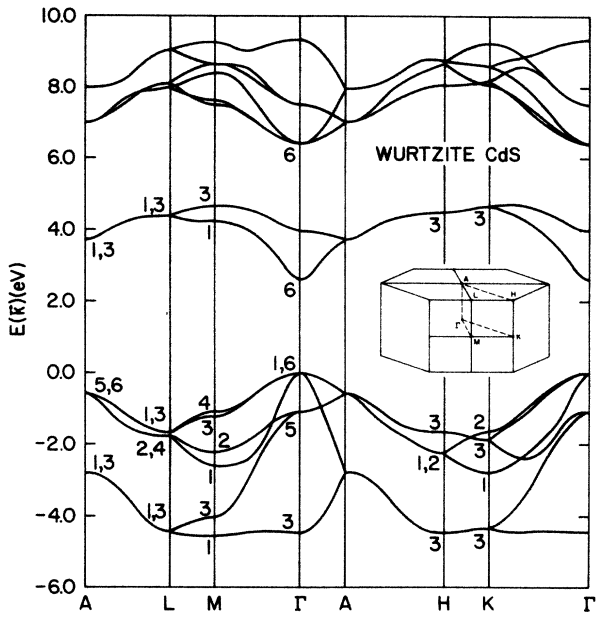

FIG. 3. Bulk-band structure of wurtzite CdS calculated from the sp^3 model. The inset shows the Brillouin zone.

reflectivity measurement[36] on wurtzite CdSe gives a transition $E(\Gamma_5^v \rightarrow \Gamma_6^c)=7.4$ eV, from which we infer that $E(\Gamma_{15}^c)=6.20$ eV. Transmission spectra[37] of epitaxially grown cubic CdSe show $E(X_5^v \rightarrow X_1^c)=6.26$ eV, and $E(L_3^v \rightarrow L_1^c)$ ranges from 4.30 to 4.65 eV. The value of $E(\Gamma_1^v)$ is unknown experimentally. To estimate it, we notice that the atomic energy of Se 4s is higher than that of S 3s by only 0.5–1.0 eV.[35] Moreover, XPS measurements[17] indicate that the Se 4s band is close to Cd 4d band. We therefore set $E(\Gamma_1^v)=-11.5$ eV.

The bulk-band structures of zinc-blende CdS and CdSe calculated from our sp^3 model are shown in Figs. 1 and 2, and those characteristic of the wurtzite structure in Figs. 3 and 4, respectively. As a final test of our model, we cal-

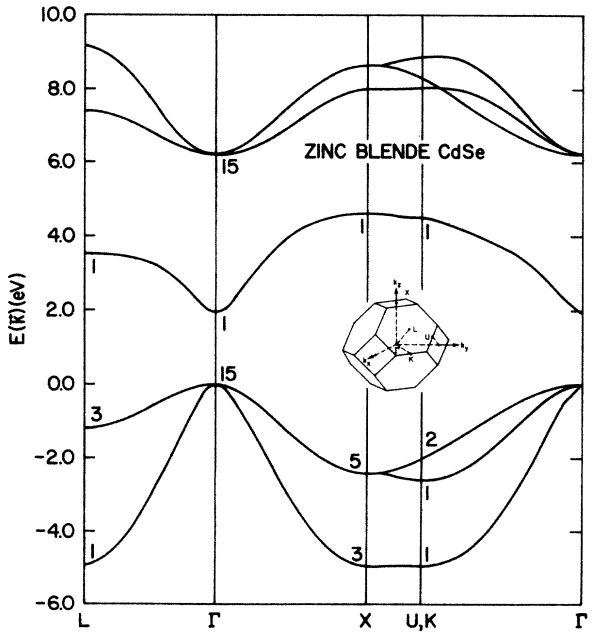

FIG. 2. Bulk-band structure of zinc-blende CdSe calculated from the sp^3 model. The inset shows the Brillouin zone.

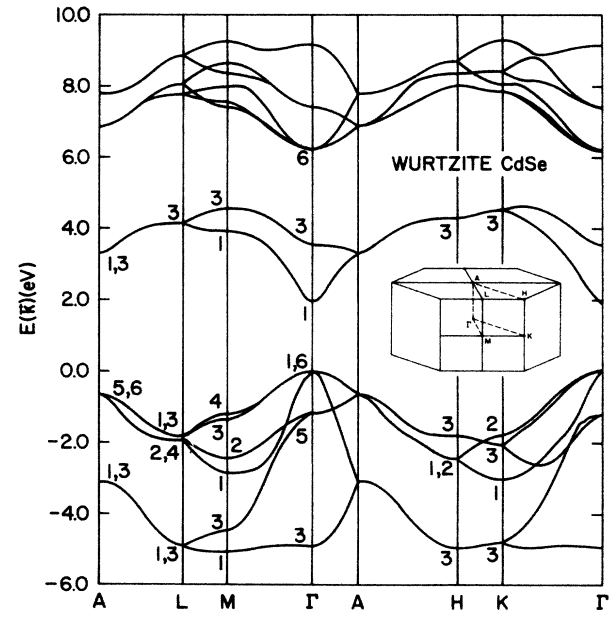

FIG. 4. Bulk-band structure of wurtzite CdSe calculated from the sp^3 model. The inset shows the Brillouin zone.

culate the bulk densities of valence states (DOVS) of wurtzite CdS and CdSe and compare them with the x-ray photoemission spectrum of the valence band.[17] The results are shown in Figs. 5(a) and 5(b) for CdS and CdSe, respectively. The agreement between the calculated DOVS and measured XPS spectra is quite good. Because we do not include final-state effects, only the peak positions can be compared.

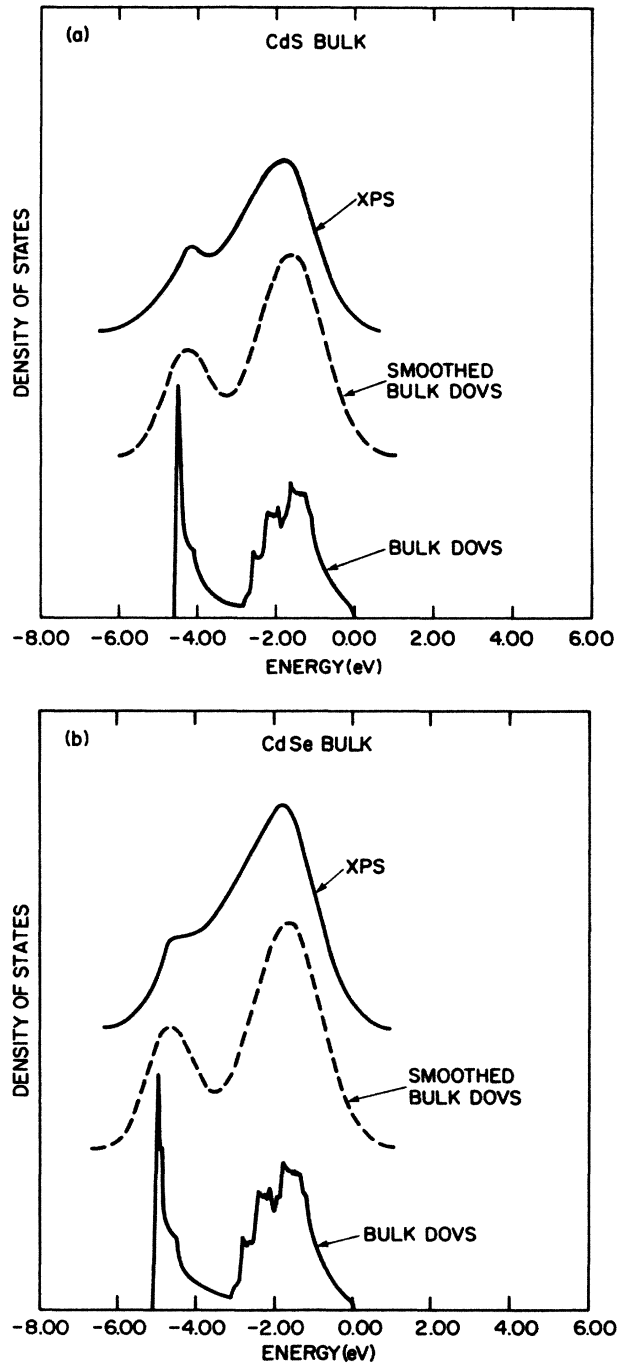

FIG. 5. DOVS calculated from the sp^3 model compared with XPS valence-band spectra of Ref. 17. The dashed curves are the convolution (by a Gaussian of width $\gamma=0.5$ eV) of the "raw" density of states. Only the peak position can be compared, because the matrix element effect is not included in the calculations. (a) CdS. (b) CdSe.

III. SURFACE ATOMIC GEOMETRIES

The surface atomic geometries are calculated using the sp^3 model determined in the previous section. We separate the total energy of the crystal into an electronic part (band energy) and an elastic part,[5] i.e.,

$$E_{\rm tot}=E_{\rm BS}+\sum_{\substack{i,j\\(i<j)}}(U_1\epsilon_{ij}+U_2\epsilon_{ij}^2)\ , \tag{10}$$

where ϵ_{ij} is the fractional change in the bond length. $E_{\rm BS}$ is the band-structure energy and is evaluated by summing the occupied states of the energy spectrum at "special points."[38,39] The parameter U_1 is determined by the equilibrium condition of the crystal,

$$U_1=-\left.\frac{\partial E_{\rm BS}}{\partial\epsilon}\right|_{\epsilon=0}\ , \tag{11}$$

in units of energy per atom. U_2 is determined by the elastic modulus, B, of the crystal,

$$2U_2=9VB-\left.\frac{\partial^2 E_{\rm BS}}{\partial\epsilon^2}\right|_{\epsilon=0}\ , \tag{12}$$

where V is the average volume of one atom. The values of U_1 and U_2 are given in Table I.

Given U_1 and U_2, we can calculate the surface atomic geometries by minimizing the total energy given by Eq. (10) or, equivalently, by sequentially reducing the Hellmann-Feynman forces on each atom in an iterative fashion. An eight-layer slab is used to simulate the semi-infinite crystal. Increasing the slab thickness does not alter our results significantly. The changes in the interatomic interactions due to the relaxation of the atoms in the top two layers are accounted for by use of the d^{-2} law[40] of the orbital interactions. In our computer program, we calculate the Hellmann-Feynman forces for each structure. The optimal surface geometry is determined by an iterative process in which the atoms are displaced by an amount proportional to the forces acting on them.[30] For the wurtzite $(10\bar{1}0)$ surface, we allow the atoms to be displaced only along y and z directions. The forces along x direction are very small due to the symmetry of the structure. For $(11\bar{2}0)$ surface, we allow relaxation along all directions. We find that the glide-plane symmetry of the undistorted unit mesh is conserved after relaxation, consistent with (LEED) results for ZnO (Ref. 41) and CdS.[42] The predicted surface structures are listed in Table III. The definitions of the surface-structure parameters are given in Figs. 6 and 7 for the wurtzite $(10\bar{1}0)$ and $(11\bar{2}0)$ surfaces, respectively.

The predicted surface geometries of CdS and CdSe are qualitatively similar to those of the corresponding zinc-based II-VI semiconductors.[4,10,13] The cations in the first layer relax inwards towards the bulk and the anions out-

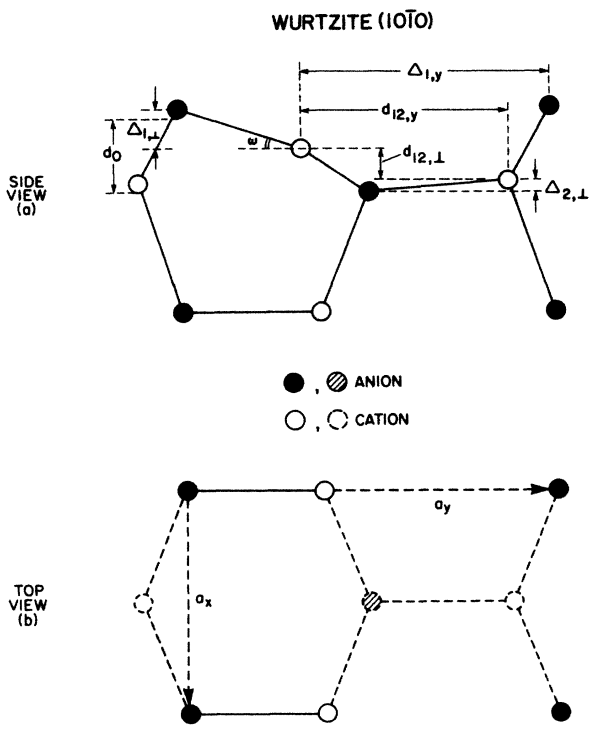

FIG. 6. (a) Side view of the surface geometry of (10$\bar{1}$0) surface. (b) The surface unit cell. The atoms in the second layer are shown by dashed circles.

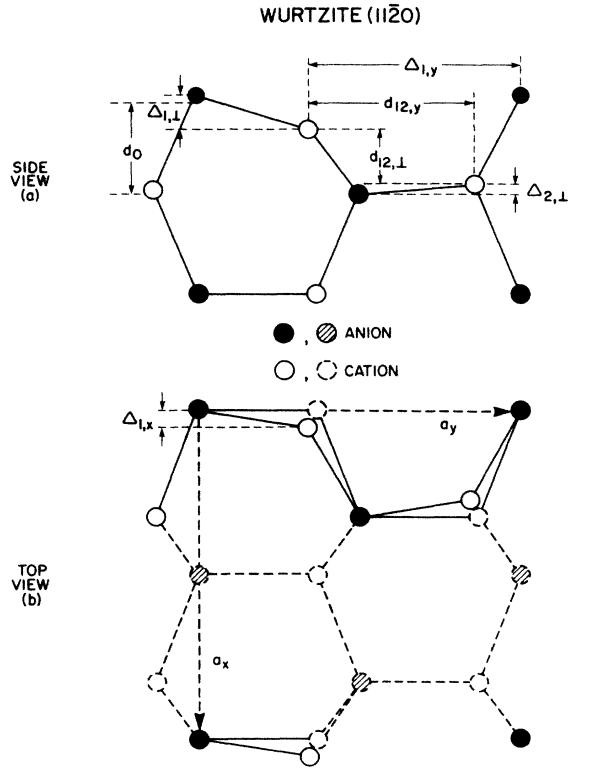

FIG. 7. (a) Side view of the surface geometry of (11$\bar{2}$0) surface. (b) The surface unit cell. The atoms in the second layer are shown by dashed circles connected by dashed bands. The undistorted unit mesh is also indicated.

wards. The perpendicular displacement of the anion relative to the cation in the top layer, characterized by $\Delta_{1,\perp}$, is 0.74 Å (CdS) and 0.78 Å (CdSe) for the (10$\bar{1}$0) surface, and is 0.68 Å (Cde) and 0.71 Å (CdSe) for the (11$\bar{2}$0) surface. The reason that the (10$\bar{1}$0) surface exhibits a larger relaxation than the (11$\bar{2}$0) surface is due to the fact that the atoms in the top layer of the (10$\bar{1}$0) surface are connected only by a single surface bond, whereas those in the (11$\bar{2}$0) surface are connected by two surface bonds.[4,10,13]

IV. SURFACE ELECTRONIC STRUCTURES

The surface electronic band structures of CdS and CdSe are shown in Figs. 8 and 9 for the (10$\bar{1}$0) and (11$\bar{2}$0) surfaces, respectively. The dot-dashed curves indicate the surface bound state S_1 of unreconstructed surfaces; the solid and dashed curves are the surface bound state and the surface resonance spectra, respectively, after relaxation.

The interpretation of the surface bound states and the surface resonances is analogous to that of the zinc based materials.[4,10,13] The state S_1 of (10$\bar{1}$0) surface (Fig. 8) originates primarily from back bonding between the top-layer anion and the second-layer cation. Its lowering towards the projected bulk-band continuum after surface reconstruction gives the major contribution to the reduction of the electronic energy. The wave function of this state is the mixture of the p component of both the anion and the cation. The state labeled S_2 in Fig. 8 is associated with the relaxation-induced localization of the p_z component of the second-layer anion; the state S_3 arises from

TABLE III. Structural parameters specifying the atomic relaxation of the (10$\bar{1}$0) and (11$\bar{2}$0) surfaces of CdS and CdSe as defined in Figs. 6 and 7, respectively. Except for ω_1, all quantities are measured in units of Å.

	a_x	a_y	$\Delta_{1,\perp}$	$\Delta_{1,y}$	$d_{12,y}$	$d_{12,\perp}$	$\Delta_{2,\perp}$	d_0	ω_1	$\Delta_{1,x}$
(10$\bar{1}$0) CdS	4.135	6.749	0.738	4.410	3.862	0.622	0.081	1.194	17.51°	
(11$\bar{2}$0) CdS	7.162	6.749	0.691	4.419	3.705	1.468	0.106	2.068		0.513
(10$\bar{1}$0) CdSe	4.300	7.020	0.775	4.593	4.036	0.639	0.065	1.241	17.71°	
(11$\bar{2}$0) CdSe	7.449	7.020	0.711	4.599	3.852	1.522	0.115	2.150		0.529

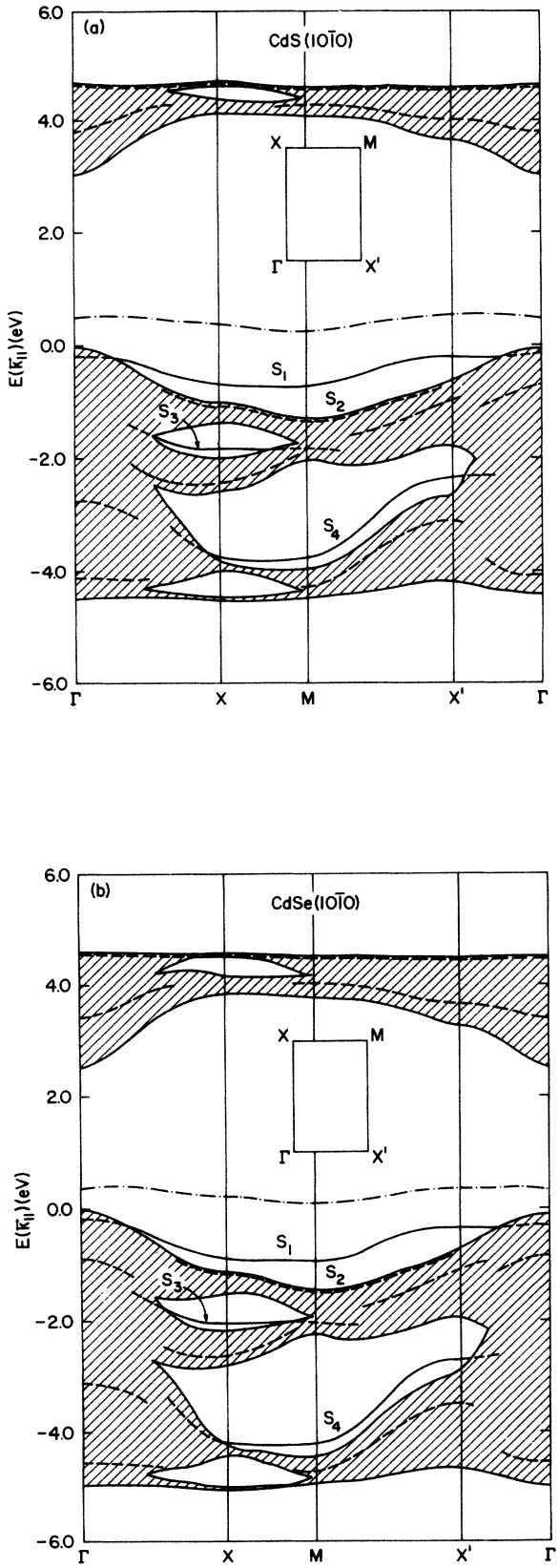

FIG. 8. Band structure of (10$\bar{1}$0) surface. The surface Brillouin zone is indicated in the inset. The state labeled S_i is described in the text. (a) CdS. (b) CdSe.

the surface bonding between the top-layer anion and cation; and the state S_4 is caused by back bonding between the s component of the first-layer cation and the p components of the second-layer anion. The driving force of the reconstruction of the (11$\bar{2}$0) surface also comes from the lowering of the state S_1 (Fig. 9) towards the bulk-band continuum.

In Fig. 10 we show the calculated first-layer (DOVS) for the (10$\bar{1}$0) surfaces, and its convolution by a Gaussian of width $\gamma=0.3$ eV (dashed curves). Also shown is the bulk DOVS (convoluted by a Gaussian of width $\gamma=0.5$ eV). The two sharp peaks near the top of the valence band in the raw DOVS comes from the surface state S_1 described above. The smaller peak corresponds to the part of S_1 near the Γ point, and the large peak to that one near the M point. The two peaks merge after convolution. Since the surface state originates from atoms in

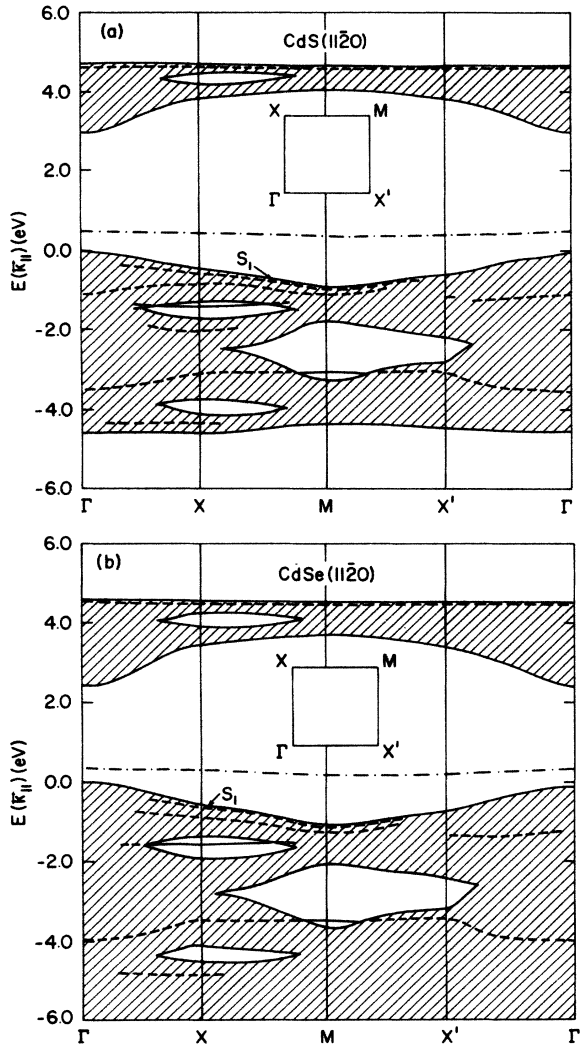

FIG. 9. Band structure of (11$\bar{2}$0) surface. The surface Brillouin zone is indicated in the inset. The state labeled S_i is described in the text. (a) CdS. (b) CdSe.

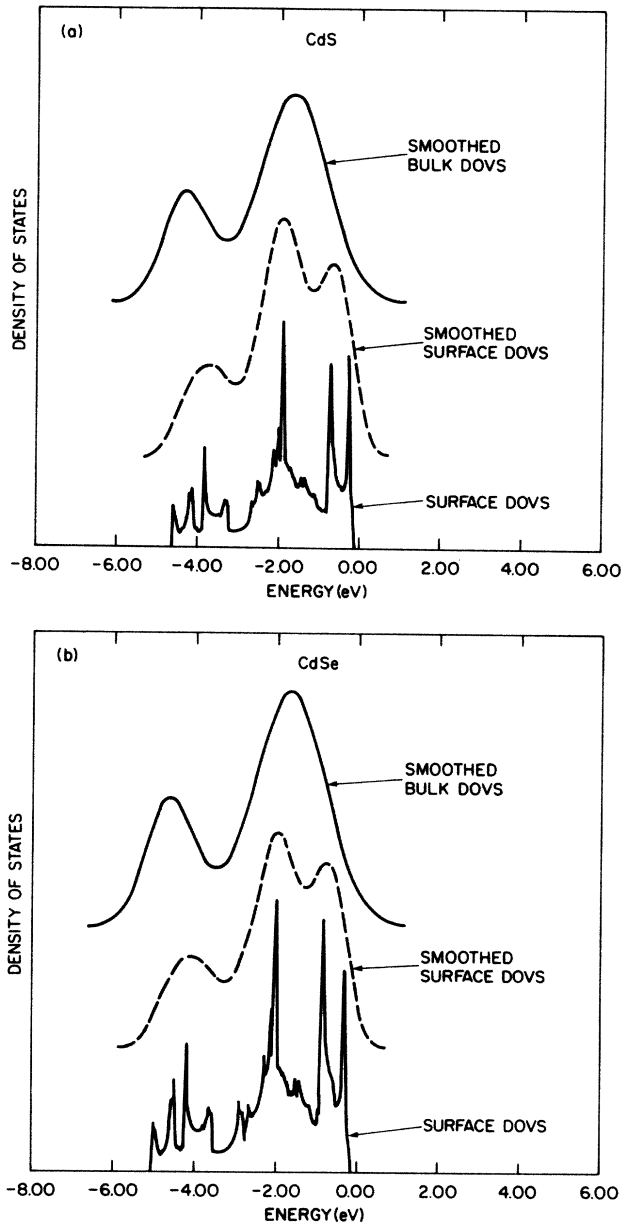

FIG. 10. First-layer density of states (DOVS) of $(10\bar{1}0)$ surface calculated from the sp^3 model. The sharp peaks near the top of the valence band are caused by the surface state S_1 in Fig. 8. The dashed curves are the convolution of the raw density of states by a Gaussian of width $\gamma=0.3$ eV. Also shown are the bulk density of states (convoluted by a Gaussian of width $\gamma=0.5$ eV). (a) CdS. (b) CdSe.

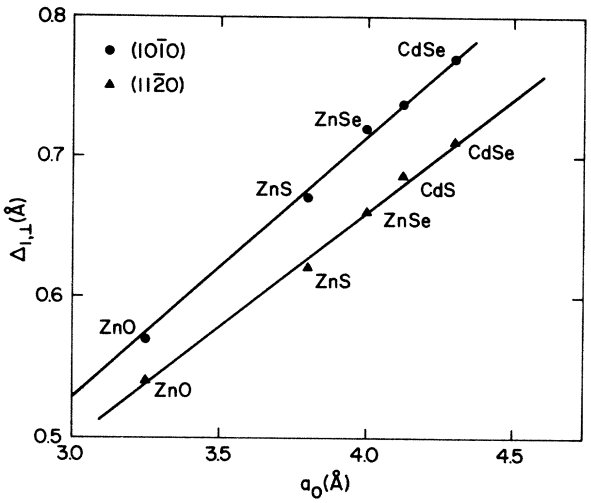

FIG. 11. Correlation between the perpendicular displacement of the top-layer anion relative to the cation, $\Delta_{1,\perp}$, and the lattice constant a_0 of the wurtzite crystal of II-VI semiconductors. The solid lines can be approximated by Eqs. (13).

the top two layers, the surface-state peak in the DOVS falls off quickly for layers further beneath the surface. For example, the DOVS of the fourth layer is almost identical to the bulk DOVS.

V. DISCUSSION

We have shown that the cleavage faces, $(10\bar{1}0)$ and $(11\bar{2}0)$, of wurtzite CdS and CdSe exhibit very similar surface reconstructions to those of zinc-based wurtzite-structure compound semiconductors. The driving force behind the surface reconstructions is the lowering of the surface state S_1 in Figs. 8 and 9 to the bulk-band continuum. This surface state is characterized by a maximum of its wave function in the first layer, and its existence should be verifiable by photoemission experiments. A preliminary report of its observation for CdSe$(10\bar{1}0)$ has been given by Duke and Wang.[43]

All the II-VI semiconductors studied so far have shown similar surface reconstructions to those of their isoelectronic III-V counterparts. To quantify this similarity, we show in Fig. 11 a plot of the perpendicular displacement of the top-layer anion relative to cation, $\Delta_{1,\perp}$, versus the lattice constant, a_0, of II-VI (wurtzite) semiconductors. It is evident from Fig. 11 that there is a strong correlation between $\Delta_{1,\perp}$ and a_0. The correlation is approximately given by

$$\Delta_{1,\perp}=0.178a_0, \quad (10\bar{1}0)\ , \tag{13a}$$

$$\Delta_{1,\perp}=0.165a_0, \quad (11\bar{2}0)\ . \tag{13b}$$

The linear relation between $\Delta_{1,\perp}$ and a_0 demonstrates that the surface relaxations of II-VI semiconductors are correlated with their bulk geometries, rather than other chemical properties (e.g., ionicity). An analogous correlation has been established for zinc-blende structure semiconductors,[44] both III-V and II-VI. Our analyses explain, therefore, why the III-V and II-VI semiconductors exhibit similar surface reconstructions, although they are so different in many chemical properties, e.g., their coordination in molecular structures.

[1]A. Kahn, Surf. Sci. Rep. **3**, 193 (1983).
[2]C. B. Duke, in *Surface Properties of Electronic Materials,* edited by D. A. King and D. P. Woodruff (Elsevier, Amsterdam, 1987), Chap. 3.
[3]P. Mark, S. C. Chang, W. F. Creighton, and B. W. Lee, Crit. Rev. Solid State Sci. **5**, 189 (1975).
[4]Y. R. Wang, C. B. Duke, and C. Mailhiot, Surf. Sci. Lett. **188**, L708 (1987).
[5]D. J. Chadi, Phys. Rev. B **19**, 2074 (1979).
[6]R. P. Beres, R. E. Allen, and J. D. Dow, Phys. Rev. B **26**, 769 (1982).
[7]C. Mailhiot, C. B. Duke, and Y. C. Chang, Phys. Rev. B **30**, 1109 (1984).
[8]A. C. Ferrez and G. P. Srivastava, J. Phys. C **19**, 5987 (1986).
[9]C. B. Duke, A. Paton, A. Kahn, and D. W. Tu, J. Vac. Sci. Technol. B **2**, 366 (1984).
[10]Y. R. Wang and C. B. Duke, Phys. Rev. B **36**, 2763 (1987).
[11]C. B. Duke, A. Paton, and A. Kahn, J. Vac. Sci. Technol. A **2**, 515 (1984).
[12]R. Z. Bachrach, R. S. Bauer, S. A. Floodström, and J. C. McMenamin, Nuovo Cimento B **39**, 704 (1977).
[13]Y. R. Wang and C. B. Duke (unpublished).
[14]C. B. Duke, R. J. Meyer, A. Paton, and P. Mark, Phys. Rev. B **18**, 4225 (1978).
[15]W. Göpel, J. Pollmann, I. Ivanov, and B. Reihl, Phys. Rev. B **26**, 3144 (1982).
[16]C. J. Vesely, R. L. Hengehold, and D. Langer, Phys. Rev. B **5**, 2296 (1972).
[17]L. Ley, R. A. Pollak, F. R. McFeely, S. P. Kowalczyk, and D. A. Shirley, Phys. Rev. B **9**, 600 (1974).
[18]C. F. Brucker and L. J. Brillson, J. Vac. Sci. Technol. **18**, 787 (1981).
[19]N. G. Stoffel, Phys. Rev. B **28**, 3306 (1983).
[20]N. G. Stoffel and G. Margaritondo, J. Vac. Sci. Technol. A **1**, 1085 (1983).
[21]K. O. Magnusson and S. A. Floodström, Phys. Rev. B **35**, 2556 (1987).
[22]M. Cardona, M. Weinstein, and G. A. Wolff, Phys. Rev. **140A**, 633 (1965).
[23]M. Cardona and G. Harbeke, Phys. Rev. **137A**, 1467 (1964).
[24]R. L. Hengehold and C. R. Fraime, Phys. Rev. **174**, 808 (1968).
[25]R. N. Euwema, T. C. Collins, D. G. Shankland, and J. S. DeWitt, Phys. Rev. **162**, 710 (1967).
[26]T. K. Bergstresser and M. L. Cohen, Phys. Rev. **164**, 1069 (1967).
[27]A. Zunger and A. J. Freeman, Phys. Rev. B **17**, 4850 (1978).
[28]K. J. Chang, S. Freyen, and M. L. Cohen, Phys. Rev. B **28**, 4736 (1983).
[29]D. J. Chadi, Phys. Rev. B **19**, 2074 (1979).
[30]C. Mailhiot, C. B. Duke, and D. J. Chadi, Surf. Sci. **149**, 366 (1985).
[31]J. L. Birman, Phys. Rev. **115**, 1493 (1959).
[32]D. J. Chadi and M. L. Cohen, Phys. Status Solidi **68**, 405 (1975).
[33]J. C. Slater and G. F. Koster, Phys. Rev. **94**, 1498 (1954).
[34]C. Sugiura, Y. Hayasi, H. Konuma, and S. Kiyono, J. Phys. Soc. Jpn. **31**, 1784 (1971).
[35]J. L. Freeouf, Phys. Rev. B **7**, 3810 (1973).
[36]R. B. Hall and H. H. Woodbury, J. Appl. Phys. **39**, 5361 (1968).
[37]R. Ludeke and W. Paul, in *Seventh International Conference on II-VI Semiconducting Compounds, Brown University, 1967,* edited by D. G. Thomas (Benjamin, New York, 1967), p. 123.
[38]D. J. Chadi and M. L. Cohen, Phys. Rev. B **8**, 5747 (1973).
[39]S. L. Cunningham, Phys. Rev. B **10**, 4988 (1974).
[40]W. A. Harrison, *Electronic Structure and the Properties of Solids* (Freeman, San Francisco, 1980).
[41]A. R. Lubinsky, C. B. Duke, S. C. Chang, B. W. Lee, and P. Mark, J. Vac. Sci. Technol. **13**, 189 (1976).
[42]S. C. Chang and P. Mark, J. Vac. Sci. Technol. **12**, 624 (1975).
[43]C. B. Duke and Y. R. Wang, in Abstracts of the 47th Conference on Physical Electronics, Pacific Grove, CA, 1987 (unpublished).
[44]C. B. Duke, J. Vac. Sci. Technol. B **1**, 732 (1983).